Received: 1 April 2022 | Revised: 5 May 2022 | Accepted: 29 May 2022

DOI: 10.1002/app.52735

RESEARCH ARTICLE

Applied Polymer SCIENCE WILEY

Modeling the through-thickness frontal polymerization of unidirectional carbon fiber thermoset composites: Effect of microstructures

Yeqing Wang

Department of Mechanical & Aerospace Engineering, Syracuse University, Syracuse, New York, USA

Correspondence
Yeqing Wang, Department of Mechanical & Aerospace Engineering, Syracuse University, Syracuse, New York 13244, USA.
Email: ywang261@syr.edu

Funding information
Syracuse University

Abstract

The frontal polymerization is a technique that creates a self-sustaining "cure front" that propagates through the thermoset resin material. Such a technique is potentially capable of substantially reducing the curing time of thermoset resin fiber composites from several hours to only a few minutes or even seconds, which is promising for the additive manufacturing and repair of thermoset fiber composites. In this study, the effect of the microstructures (i.e., fiber volume fraction, fiber tow size, and fiber tow shape) of unidirectional fiber composites on the frontal polymerization initiated in the through-thickness direction of the composites is investigated through computational modeling. The computational model is verified through comparisons with experimental data. The simulation results show that the frontal polymerization process is largely affected by the fiber volume fraction and the fiber tow shape and is insensitive to the fiber tow size. The average front velocity decreases significantly as the fiber volume fraction increases from 0% to 30% and then decreases mildly from 30% to 46%. Above 46%, the average front velocity plateaus. Moreover, the average front velocity decreases in an approximately linear fashion as the ratio between the major radius and minor radius of the elliptical cross section of fiber tow increases.

KEYWORDS

additive manufacturing, carbon fiber composites, frontal polymerization, microstructure, thermoset composites

1 | INTRODUCTION

Thermoset-matrix fiber composites, such as carbon fiber reinforced epoxy composites, are increasingly used for applications in a variety of industries (e.g., aerospace, marine, automotive, energy, civil infrastructure, high-end sports) due to their significant weight saving capability and extraordinary properties, such as the high specific stiffness and strength, and excellent fatigue and corrosion resistances. However, these composites require crosslinking for curing and consolidation in the manufacturing process, which is time consuming and can often take several hours. For example, the complete cure cycle of the Solvay CYCOM 977–3 epoxy resin will take about 10 h in an autoclave.[1] Such a long curing time significantly hinders the additive manufacturing and repair of such composites. Additionally, a large autoclave is a major capital investment for any composite structure manufacturers, for example, a 14-meter diameter by 27-meter-long autoclave could cost on the order of $40 million to build and $60 million to install, not to mention the high cost of

operation (nitrogen gas and power).[2] Meanwhile, the energy consumption will lead to adverse environmental impacts. For example, the autoclave curing process results in about 75 kg CO_2 equivalent emission for each carbon fiber reinforced polymer matrix composite panel (400 × 400 × 4 mm).[3]

The major challenges in the additive manufacturing and repair of thermoset-matrix fiber composites are the extensive curing time as well as the immense energy associated with high temperature and pressure. The frontal polymerization technique is one of the trending techniques among various methods (e.g., reactive extrusion,[4] microwave curing,[5] UV photocuring,[6] pre-print or post-print oven curing[7–10]) to address these challenges. Specifically, the frontal polymerization is a self-propagation reaction caused by exothermic polymerization, where a "cure front" is formed by a local thermal stimulus that propagates through the material.[11–14] This technique can reduce the curing time from several hours to only a few seconds and does not rely on the autoclave or oven, which significantly reduces the energy consumption and the overall cost. The success of using the frontal polymerization technique has been demonstrated for many thermoset monomers, such as the acrylate and epoxy resin monomers.[15–17] For example, researchers from Vienna University of Technology (Austria) successfully cured the epoxy monomer and epoxy composites with high filler contents of up to 74 vol% glass microspheres and 40 vol% short carbon fibers using the radical induced cationic frontal polymerization procedure.[18] The complete curing of their glass microspheres specimens (50 × 10 × 10 mm) took approximately 28 s. Their experimental test results showed that the tensile properties of the epoxy composite specimens cured using the frontal polymerization are comparable to those cured using conventionally methods. Moreover, researchers from the University of Illinois modeled the frontal polymerization of unidirectional carbon fiber composites in the fiber direction through formulating a thermo-chemical model.[19,20] The evolution of the temperature and the degree of the cure were investigated using a reaction–diffusion model with finite element analysis. The model uses a simplification strategy by homogenizing the fiber and matrix, which was employed to study the effect of fiber volume fractions on the overall curing performance. Their simulation results indicate that the velocity of the curing front (i.e., front velocity) initially increases as the fiber volume fraction increases from 0% to 15% and then decreases as the fiber volume fraction continues to increase, when the frontal polymerization is triggered along the fiber direction of carbon fiber thermosetting dicyclopentadiene (DCPD) composite specimens. The trend is believed to be caused by the competing mechanism between the heat diffusion in the carbon fibers and the exothermic heat generation. Recently, researchers have also experimentally and numerically demonstrated that the front velocity can be enhanced by introducing thermally conductive elements, such as aluminum and copper strips.[21,22]

Currently, the research is still far from maturity for using the frontal polymerization technique to cure thermoset-matrix fiber composites, especially for composites with opaque and thermally conductive fibers or particles, such as the carbon fiber, carbon nanotubes, and graphene nanoplatelets. Specifically, the effect of the microstructures of fiber composites, such as the fiber volume fraction, fiber tow size, and the shape of the fiber tow cross sections, on the frontal polymerization of composites, especially when triggered along the through-thickness direction of the fiber composites remain largely unexplored.

In this study, computational studies are conducted based on the reaction–diffusion model to examine the effect of the microstructures on the through-thickness frontal polymerization of unidirectional carbon fiber composites. The computational model is created in a two-dimensional configuration. The carbon fibers and the resin of the composite material are modeled as separate geometric domains. When compared to existing modeling approach of homogenizing the fiber and matrix,[19,23] this approach allows us to capture the detailed effect of microstructural features on the frontal polymerization process. The model is implemented using finite element analysis with user subroutines and is verified by comparing against experimental data. After verification, the model is employed to study the effect of microstructures, including the fiber volume fraction, fiber tow size, and fiber tow shapes, on the frontal polymerization of the unidirectional fiber composites. Note that this study focuses on the frontal polymerization that is initiated in the through-thickness direction of the fiber composites. This is because the through-thickness curing is arguably more compatible with the additive manufacturing of fiber composites, such as the automated tape laying and the automated fiber placement additive manufacturing process. The results are expected to provide insights into the scale-up of the frontal polymerization technology for the manufacturing and repair of thermoset fiber composites.

2 | MATHEMATICAL FORMULATION

The heat transfer in the thermoset resin due to the initiation and propagation of the frontal polymerization is governed by the classical heat condition equation, where the heat is produced due to the enthalpic reaction. The equation is written as,

$$\nabla \cdot (k\nabla T) + \rho H_r \frac{\partial \alpha}{\partial t} = \rho C_p \frac{\partial T}{\partial t}, \quad (1)$$

TABLE 1 Material properties and curing kinetics parameters of the DCPD resin[20]

Material properties	**Density**	$\rho = 980$ kg/m^3
	Thermal conductivity	$k = 0.15$ W/m·K
	Specific heat	$C_p = 1600$ J/kg·K
	Total enthalpy of reaction	$H_r = 350$ J/g
Curing kinetics parameters	Pre-exponential coefficient	$A = 8.55e15$ 1/s
	Activation energy	$E = 116.75$ kJ/mol
	Orders of reaction	$n = 1.72$ and $m = 0.77$
	Diffusion parameters	C = 14.48 and $\alpha_C = 0.41$

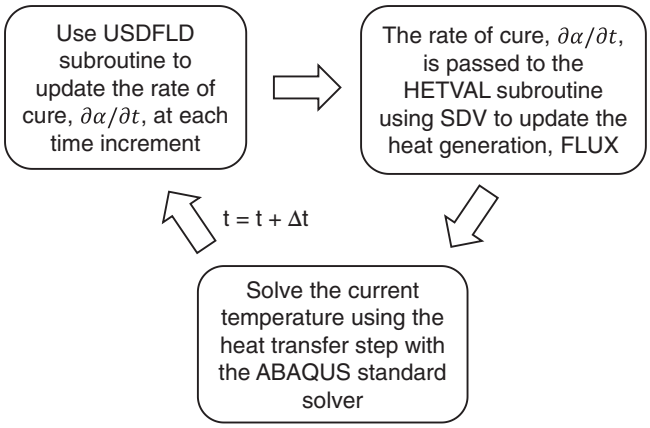

FIGURE 1 Flowchart of the numerical implementation for modeling the frontal polymerization using ABAQUS with HETVAL and USDFLD subroutines.

where k is the thermal conductivity, C_p is the specific heat, ρ is the density, H_r is the total enthalpy of reaction, and T and α are the temperature and the degree of cure, respectively. Here, the rate of the cure, $\partial\alpha/\partial t$, is described using the Arrhenius equation and the classical Prout-Tompkins (PT) autocatalytic model,

$$\frac{\partial \alpha}{\partial t} = A\exp\left(-\frac{E}{RT}\right)(1-\alpha)^n \alpha^m \frac{1}{1+\exp[C(\alpha-\alpha_C)]}, \quad (2)$$

where A, E, n, m, C, and α_C are curing kinetics parameters. They are typically obtained from Differential Scanning Calorimetry experiments by fitting the evolution of the rate of the cure. In this study, we consider the DCPD resin. The reason is due to the availability of the required material properties of the DCPD resin for modeling, including the thermal properties, enthalpy of reaction, and the curing kinetics parameters[20] (Table 1), as well as the availability of the experimental data of frontal polymerization[20] for model validation (see Section 4). The DCPD resin is best known for its fast curing and ease of processing with a low viscosity in the monomer state. DCPD-based composites are usually used for applications, such as automotive bumpers and heavy equipment bodies.[24] As reported in Reference 20, the void content of the DCPD composites manufactured using frontal polymerization is 0.15%, which is even lower than that of the conventionally cured DCPD composites (1.30%). Due to the small void content, its effect on the material properties and curing kinetics is considered negligible. Note that in Equation (2), the term $(1-\alpha)^n\alpha^m$ reflects the classical PT model, where n and m are the orders of reaction. Such a term is augmented by a diffusion factor, that is, $(1+\exp[C(\alpha-\alpha_C)])^{-1}$, where the constants C and α_C are used to model the diffusion at higher temperatures.[19]

3 | NUMERICAL IMPLEMENTATION

The mathematical formulations described in Section 1 are numerically implemented using ABAQUS, that is, a commercial, general-purpose finite element analysis (FEA) software. Note that the built-in heat transfer step of ABAQUS only allows us to model general heat transfer problems that do not involve complicated internal heat generations. In the case of the frontal polymerization, the heat is generated from the enthalpic reaction, which cannot be directly defined in the ABAQUS input file. To accommodate this, a heat flux subroutine (i.e., HETVAL) is developed. Additionally, a user field subroutine (i.e., USDFLD) is developed to update the rate of cure, $\partial\alpha/\partial t$, at each integration point and at each time increment. The updated rate of cure is then saved as a solution-dependent state variable (i.e., SDV) and then passed to the HETVAL subroutine to update the volumetric heat flux at each time increment. Figure 1 shows the flowchart of the numerical implementation that involves the HETVAL and USDFLD subroutines. These subroutines will be made available on the author's lab website http://composites.syr.edu/ upon publication.

4 | MODEL VERIFICATION

Before employing the proposed finite element model to study the effect of the microstructure of the unidirectional fiber composites on the frontal polymerization

process, the model is verified by comparing predictions against the experimental test data.[20] In the experiments, a glass test tube with a radius of 5.5 mm and a wall thickness of 1 mm is filled with the DCPD resin. A single 3 K carbon fiber tow (i.e., containing 3000 individual carbon fiber filaments) is placed at the center of the glass tube. The frontal polymerization is initiated using a soldering iron on the left side (i.e., opening side) of the glass tube. Such an external heat source was carefully applied to ensure that the heat only affects the monomer and did not get in contact with the fiber tow to avoid the direct diffusion of the heat through the fiber tow. Note that the problem with the glass tube is essentially symmetric along the center axis and, hence, a two-dimensional axisymmetric computational domain is created to reduce the computational cost. Figure 2 depicts the problem configuration.

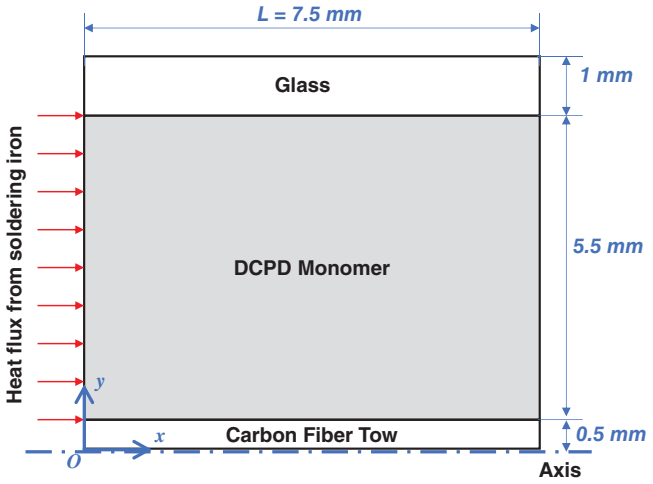

FIGURE 2 The configuration of the problem used for the model verification. [Color figure can be viewed at wileyonlinelibrary.com]

To replicate the experimental testing conditions, the following initial and boundary conditions are applied in the finite element model:

$$T|_{t=0} = T_0, \text{ and } \alpha|_{t=0} = \alpha_0, \tag{3}$$

$$T|_{x=0, 0 \le t \le t_{trig}} = T_{trig}, \tag{4}$$

$$\left.\frac{\partial T}{\partial x}\right|_{x=0, t > t_{trig}} = 0 \text{ and } \left.\frac{\partial T}{\partial x}\right|_{x=L} = 0 \tag{5}$$

where Equation (3) denotes the initial temperature and initial degree of cure that are applied, with $T_0 = 23^{\circ}$C and $\alpha_0 = 0.07$.[20] Equation (4) describes that a triggering temperature, T_{trig}, is applied on the left side (i.e., the opening) of the glass tube for a duration of t_{trig}, with $T_{trig} = 210^{\circ}$C and $t_{trig} = 7$ s.[20] Equation (5) describes that thermal insulation boundary conditions are applied on the right side of the glass tube during the entire simulation and on the left side of the glass tube after the triggering heat source is removed, respectively.

TABLE 2 Material properties and curing kinetics parameters of the DCPD resin.[20]

	Density	**1760 kg/m^3**
	Thermal conductivity	**10.45 W/m·K**
Carbon fiber	**Specific heat**	**795 J/kg·K**
Glass	Density	2230 kg/m^3
	Thermal conductivity	1.14 W/m·K
	Specific heat	800 J/kg·K

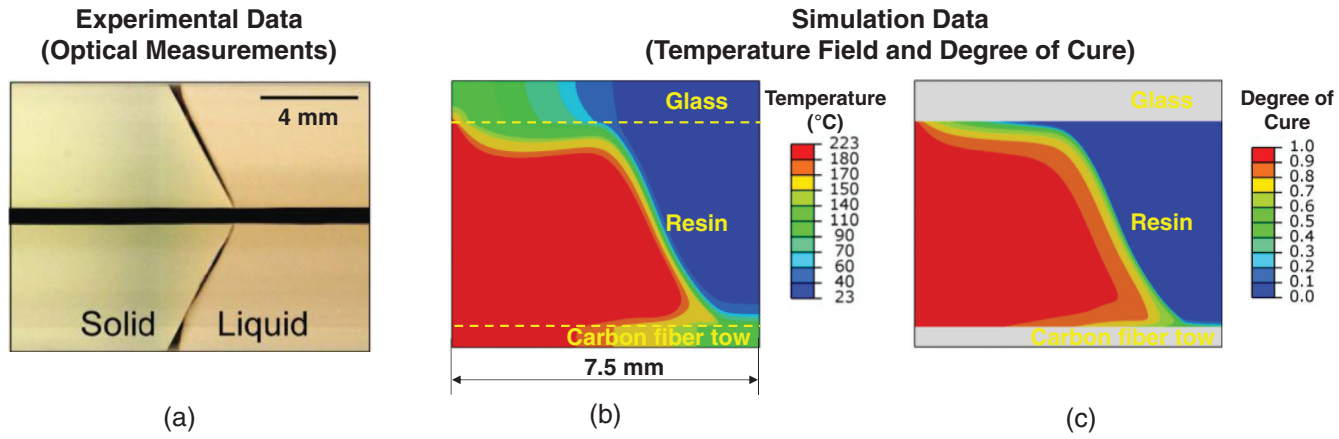

FIGURE 3 Comparison between experimental data and simulation data for frontal polymerization of DCPD resin containing a single carbon fiber tow: (a) optical measurement, (b) predicted temperature field, and (c) predicted degree of cure, all at 5.5 s. [Color figure can be viewed at wileyonlinelibrary.com]

The computational domain is meshed using the 4-node linear axisymmetric heat transfer quadrilateral elements in ABAQUS (i.e., DCAX4). An extremely fine mesh with an element size of 0.02 × 0.02 mm is used for the domain of the DCPD monomer while a coarse mesh with an element size of 0.10 × 0.02 mm is used for the domains of the glass and the carbon fiber tow. Note that it is critical to use extremely fine mesh for the DCPD monomer domain to capture the rate of the cure, as specified in Equation (2). A mesh dependence study has been conducted in prior, and the results indicate that convergence has been achieved when using an element size of 0.02 × 0.02 mm. The meshing has resulted in a total of 99,375 elements. The computation is performed on a laptop with dual core and 16 GB RAM. The computational time is about 1.5 h.

The material properties and the curing kinetics parameters of the DCPD monomer are same as those listed in Table 1. Note that the actual thermal conductivity could experience slight variations during the curing process. For example, the thermal conductivity of the RTM6 resin increases from 0.19 to 0.23 W/m·K, when the degree of cure rises from 5% to 70%.[25] However, the experimental data for the degree-of-cure dependent thermal conductivity is not available for DCPD resin, and thus, this effect is ignored in our simulation studies. The evolutions of the temperature field and the degree of cure of the DCPD monomer, as well as the evolution of the temperature in the carbon fiber tow and the glass tube wall are predicted using the model. The thermophysical properties of the carbon fiber tow and the glass are listed in Table 2.

Figure 3 illustrates the comparison between the experimental data and the simulation data. As we can see, the predicted cure front matches the optical measurements[20] reasonably well. The average velocity of the polymerization front is 1.07 mm/s, which is in good agreement with the experimental data.[20] Furthermore, the maximum temperature predicted from the simulations is 223°C, which also agrees very well with the experimental data.[20] Overall, the numerical implementation realized by the HEATVAL and USDFLD subroutines of the finite element model is considered to be validated, with a capability to predict the dynamic evolution of the temperature and the degree of cure during the frontal polymerization.

5 | RESULTS AND DISCUSSIONS: EFFECT OF MICROSTRUCTURE ON THE FRONTAL POLYMERIZATION OF UNIDIRECTIONAL CARBON FIBER COMPOSITES

After the model is verified, it was employed to study the effect of the microstructures of the unidirectional carbon

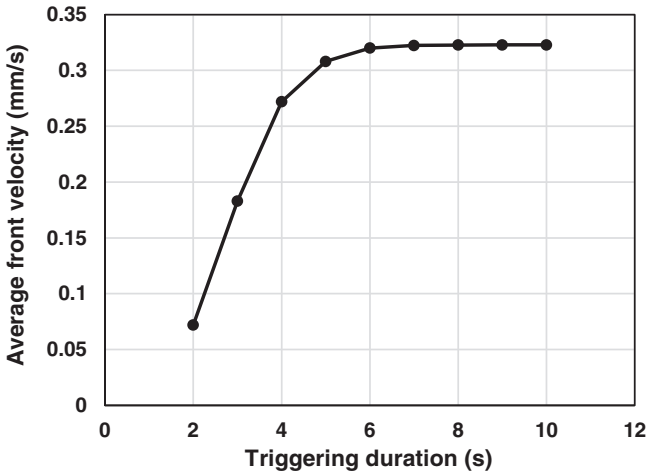

FIGURE 5 The effect of the duration of the triggering temperature on the predicted average front velocity.

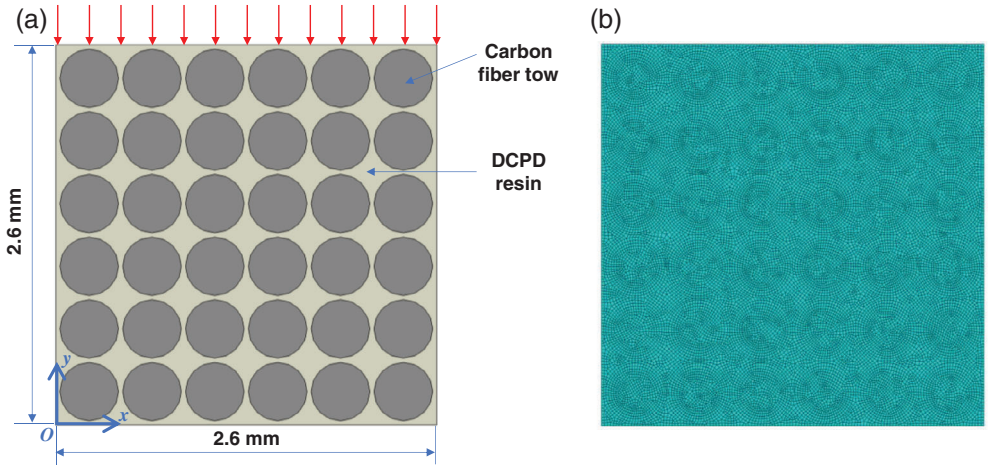

FIGURE 4 Problem configuration of the frontal polymerization in unidirectional carbon fiber DCPD resin composites. [Color figure can be viewed at wileyonlinelibrary.com]

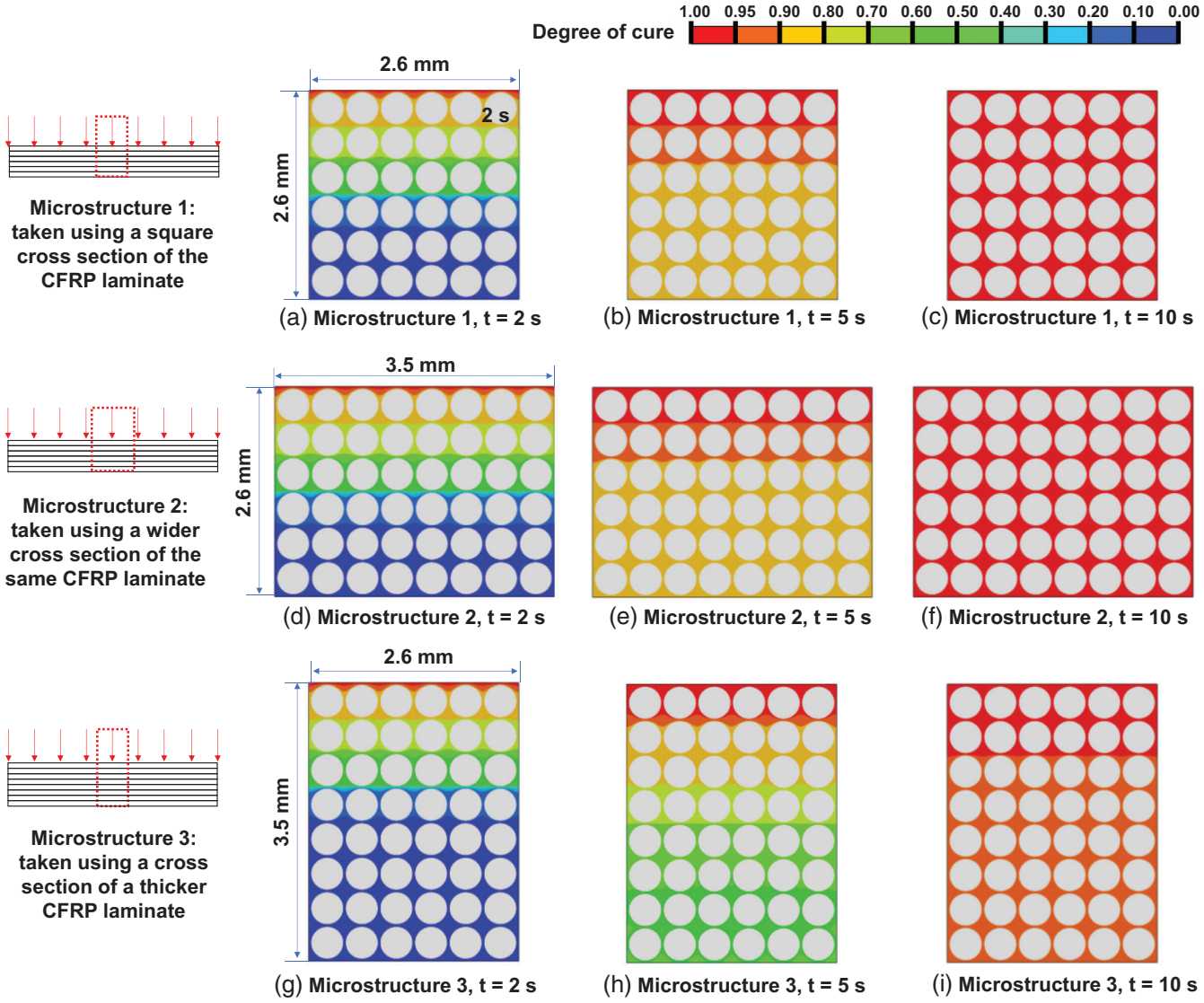

FIGURE 6 Comparison of the predicted degree of cure in microstructures with different domain sizes and a fixed V_f of 67% during the frontal polymerization at different times (2, 5, and 10 s). [Color figure can be viewed at wileyonlinelibrary.com]

fiber composites on the frontal polymerization process. The plane of isotropy of the unidirectional composite (i.e., the 2–3 plane of the composite laminate) is chosen as the computational domain since the current study focuses on the frontal polymerization in the through-thickness direction. To reduce the computational costs, the fiber tow containing a number of individual fibers is assumed to have a circular cross section. Such an assumption has also been used in the study of investigating the effect of fiber diameter and fiber bundle count on the resin transfer molding process of carbon fiber composites.[26] The radius of the circular fiber tow is calculated using the areas of the cross section of the fiber tow in different tow sizes. For HexTow AS4 carbon fiber, the radii are 0.195, 0.276, and 0.391 mm, for 3 K, 6 K, and 12 K fiber tows, respectively.[27] Note that, the effect of the fiber tow cross-sectional shape (circular vs. elliptical) is also studied in this paper and the results are discussed in Section 5.4.

Figure 4 illustrates the problem configuration. The computational size is 2.6 × 2.6 mm. Note that the effect of the computational size is discussed in Section 5.1. The bottom and vertical surfaces are assumed to be thermally insulated. To trigger the frontal polymerization across the thickness direction, the top surface of the composite is applied with a triggering temperature of $T_{trig} = 210^{\circ}\mathrm{C}$ for 5 s.

Note that the duration of the triggering temperature also affects the frontal polymerization process. Figure 5 shows the predicted average front velocity vs. the triggering duration. Here, the average front velocity is the ratio between the thickness and the total duration used for

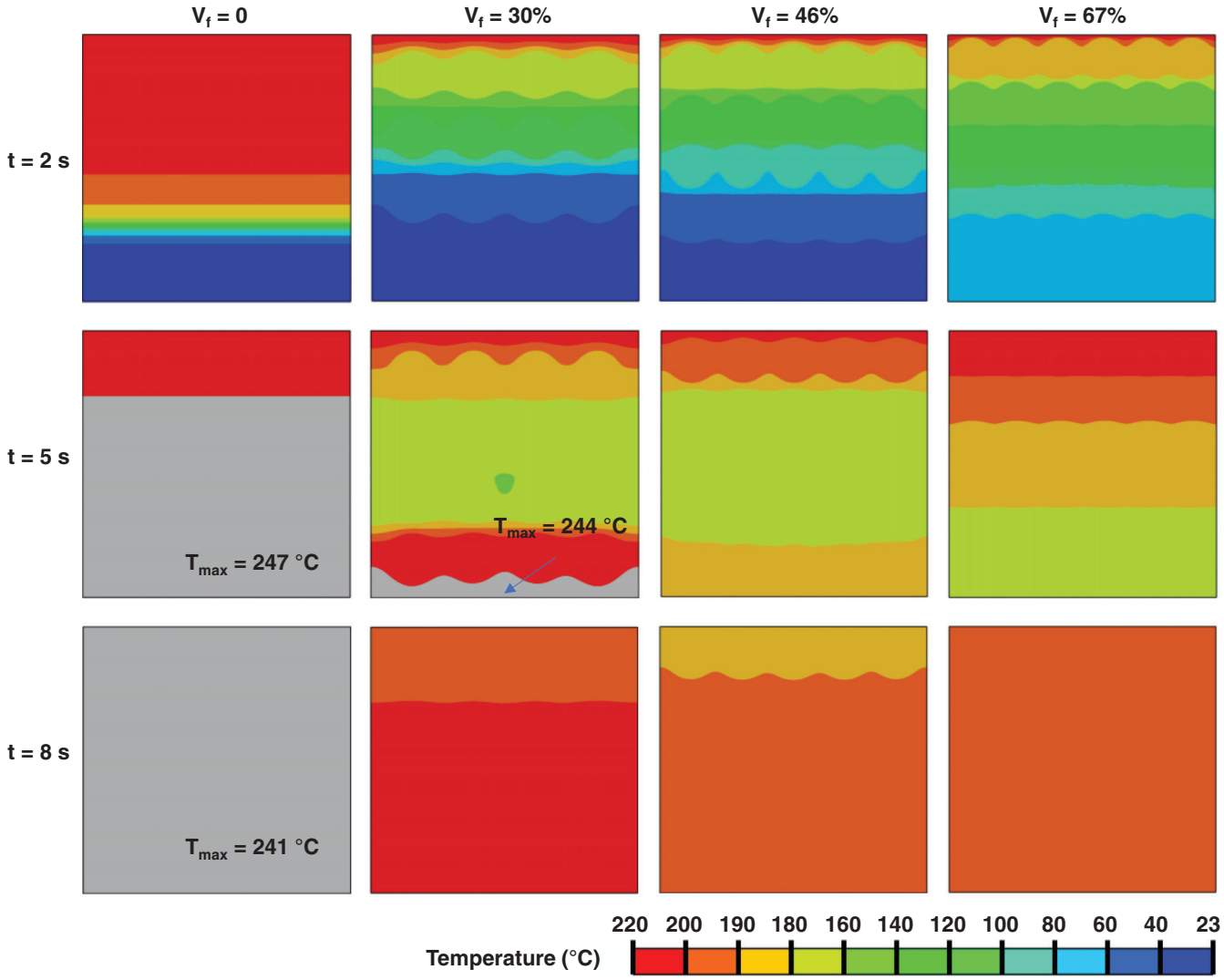

FIGURE 7 Comparison of the evolutions of the temperature field for unidirectional fiber composites with different fiber volume fractions (the gray color represents temperatures higher than 220°C). [Color figure can be viewed at wileyonlinelibrary.com]

curing the entire microstructure. We can see that the average front velocity rapidly increases from 0.072 to 0.32 mm/s as the triggering duration increases from 2 to 6 s. Such an acceleration saturates when the duration exceeds 6 s due to the sufficient heat generation within the material for activating the frontal polymerization process. A short triggering duration only heats up the surface of the composite while the in-depth region remains relatively cool, and thus, such a condition requires longer time for the heat to travel through the material to activate the polymerization process. Contrarily, a longer triggering duration allows the heat to travel deeper into the material, thereby allowing a larger extent of material to quickly activate the polymerization process. In the following studies, a triggering duration of 5 s is used for all simulations for consistency.

5.1 | Effect of computational size

Simulation results in Figure 6 illustrates the effect of the computational sizes on the frontal polymerization at different times (2, 5, and 10 s). Specifically, row 1 shows the results for a microstructure with a size of 2.6 × 2.6 mm, row 2 shows the results for a wider microstructure, that is, 3.5 × 2.6 mm, and row 3 shows the results for a thicker microstructure, that is, 2.6 × 3.5 mm (which represents a thicker laminate). For all three cases, the fiber volume fraction is fixed at 67%. The comparison of results between row 1 and row 2 shows that increasing the width of the microstructure does not have any effects on the polymerization process. This is expected since the microstructure represents a small portion extracted from the composite laminate across the thickness (see leftmost

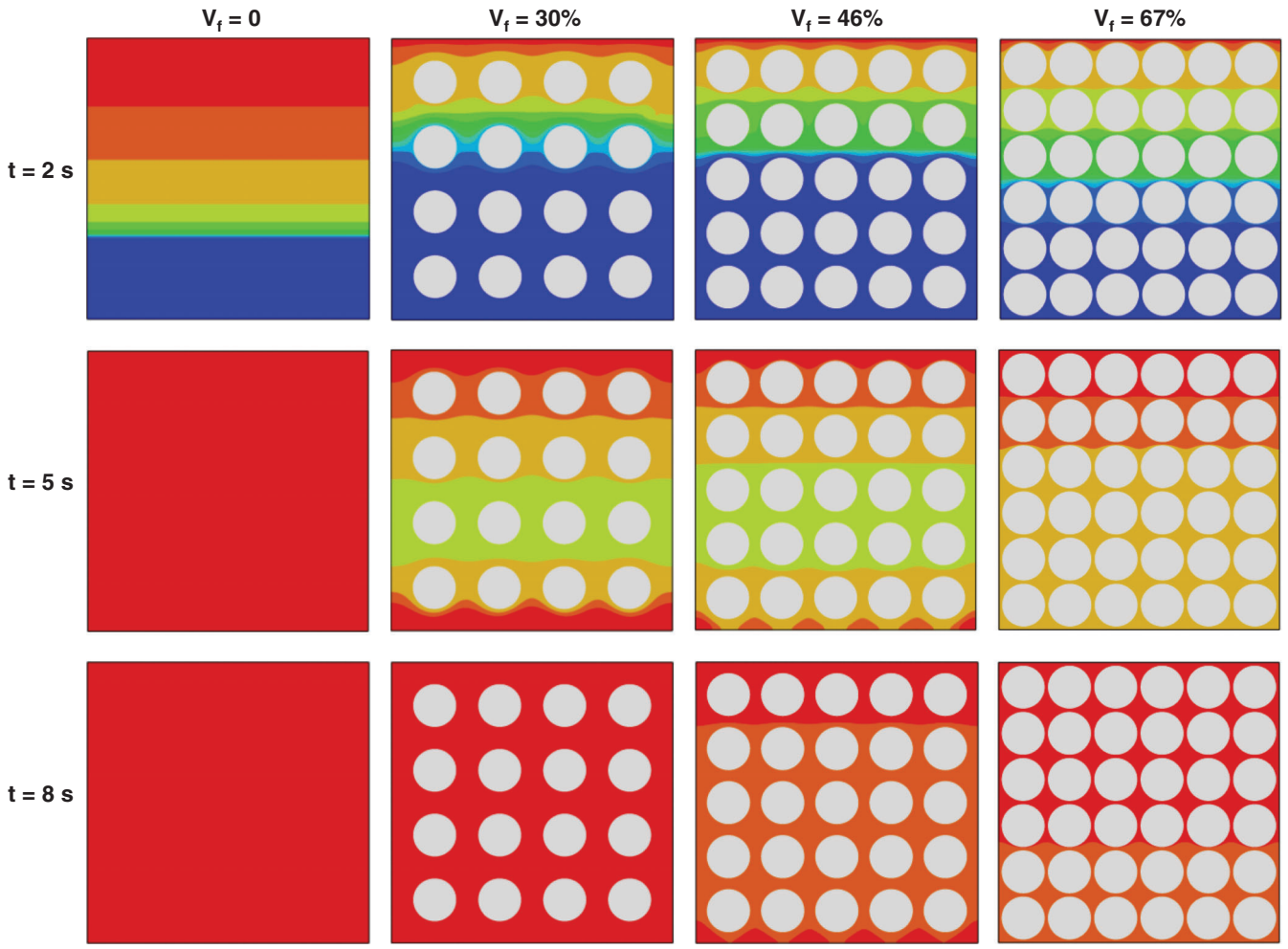

FIGURE 8 Comparison of the evolutions of the degree of cure field for unidirectional fiber composites with different fiber volume fractions (the color legend is same with the one in Figure 6, where red denotes fully cured while blue denotes uncured). [Color figure can be viewed at wileyonlinelibrary.com]

schematics in rows 1 and 2 of Figure 6), where the triggering temperature is uniformly applied over the entire top surface. The comparison of results between row 1 and row 3 demonstrates that increasing the thickness of the microstructure leads to significant changes in the frontal polymerization process. Specifically, the average front velocity decreases significantly from 0.32 to 0.060 mm/s as the thickness of the microstructure increases from 2.6 to 3.5 mm. In the following simulation studies, a computational size of 2.6 × 2.6 mm is used for consistency.

5.2 | Effect of fiber volume fraction

The effect of the fiber volume fraction on the frontal polymerization of the unidirectional fiber composites in the through-thickness direction is shown in Figures 7 and 8. Specifically, Figure 7 provides the comparison of the evolution of the temperature fields at different times (2, 5, and 8 s) while Figure 8 provides the corresponding comparison of the evolution of the degree of cure. It can be seen, at $V_f = 0$ (i.e., pure DCPD resin), the heat quickly transfers from the top to the bottom. Moreover, as the temperature quickly rises, the rate of the cure, that is, $\partial\alpha/\partial t$, also significantly increases (see Equation (2)), which leads to the rapid volumetric heat generation due to enthalpic reaction, that is, $\rho H_r \partial\alpha/\partial t$. At 5 and 8 s, the maximum temperature reaches 247 and 241°C, respectively, which are both found at the bottom of the composites. Then, the heat at the bottom transfers back to the top, which results in a "bottom-to-top" frontal polymerization in the through-thickness direction. This "bottom-to-top" frontal polymerization can also be found for composites with fiber volume fractions of 30% and 46% (see the second and third column of Figure 8). The two polymerization fronts propagate to meet up as one of them traveling from the top to the bottom and the other

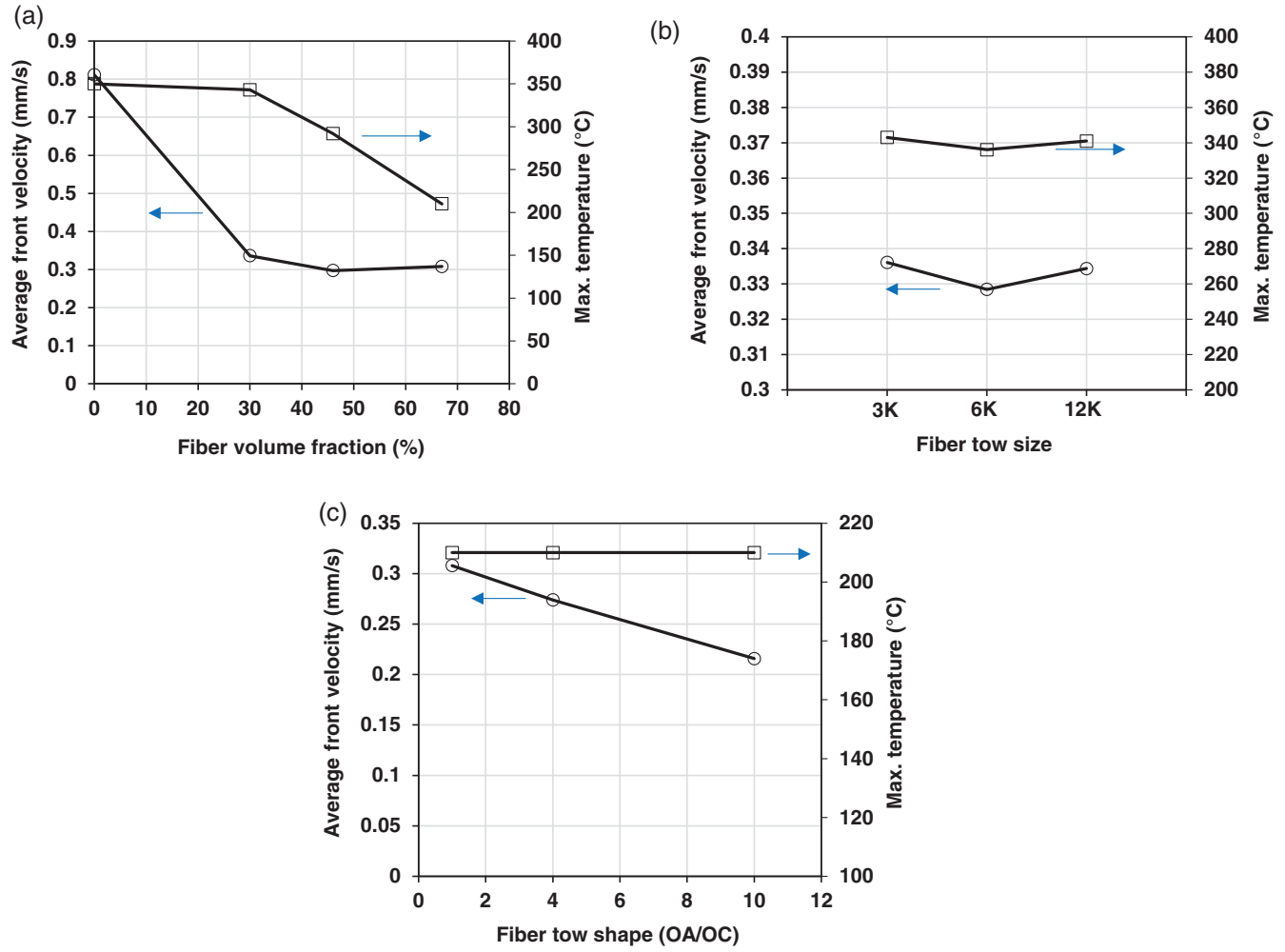

FIGURE 9 The effect of fiber volume fraction (a), fiber tow size (b), and fiber tow shape (c) on the average front velocity and the maximum temperature in frontal polymerization process. [Color figure can be viewed at wileyonlinelibrary.com]

one traveling from the bottom to the top. As the fiber volume fraction increases, this "bottom-to-top" frontal polymerization phenomenon becomes less noticeable. This is because more volumetric heat is consumed through the conduction within the thermally conductive fibers, which counters the temperature increase in the monomer. As shown in Figures 7 and 8, the "bottom-to-top" frontal polymerization can no longer be found for the composite with a V_f of 67%.

Overall, the maximum temperature during the polymerization drops as the fiber volume fraction increases. As shown in Figure 9a, for composites with relatively lower fiber fractions (0%, 30%, and 46%), the maximum temperatures are much higher than the triggering temperature (210°C), whereas for composites with a high fiber fraction (67%), the maximum temperature stays the same as the triggering temperature. Moreover, as shown in Figure 9a, the average front velocity initially experiences a significant drop from 0.81 to 0.34 mm/s (i.e., a 58.0% reduction) as the V_f increases from 0% to 30%. Then, the average front velocity undergoes a slight reduction from 0.34 to 0.30 mm/s (i.e., a 11.8% reduction) as the V_f increases from 30% to 46%. When the V_f gets above 46%, the average front velocity plateaus. Note that this finding should not be confused with the finding reported by Goli et al.,[19] where they focused on the frontal polymerization triggered along the fiber direction and reported that the front velocity in the fiber direction increases first as the V_f increases from 0% to 15% and then continuously decreases when V_f increases to above 15%,[19] whereas this study focuses on the frontal polymerization triggered in the through-thickness direction. This infers that the anisotropicity of the fiber composites leads to complex frontal polymerization behaviors in different directions, which reflects the necessity of this study and the importance of the current findings for providing guidance in the scale-up of this technology for practical applications, such as the manufacturing of multidirectional fiber composite laminates and novel multiphase composites that contain nanofillers (e.g., carbon nanotube, graphene nanoplatelets) for performance enhancements.[28–31]

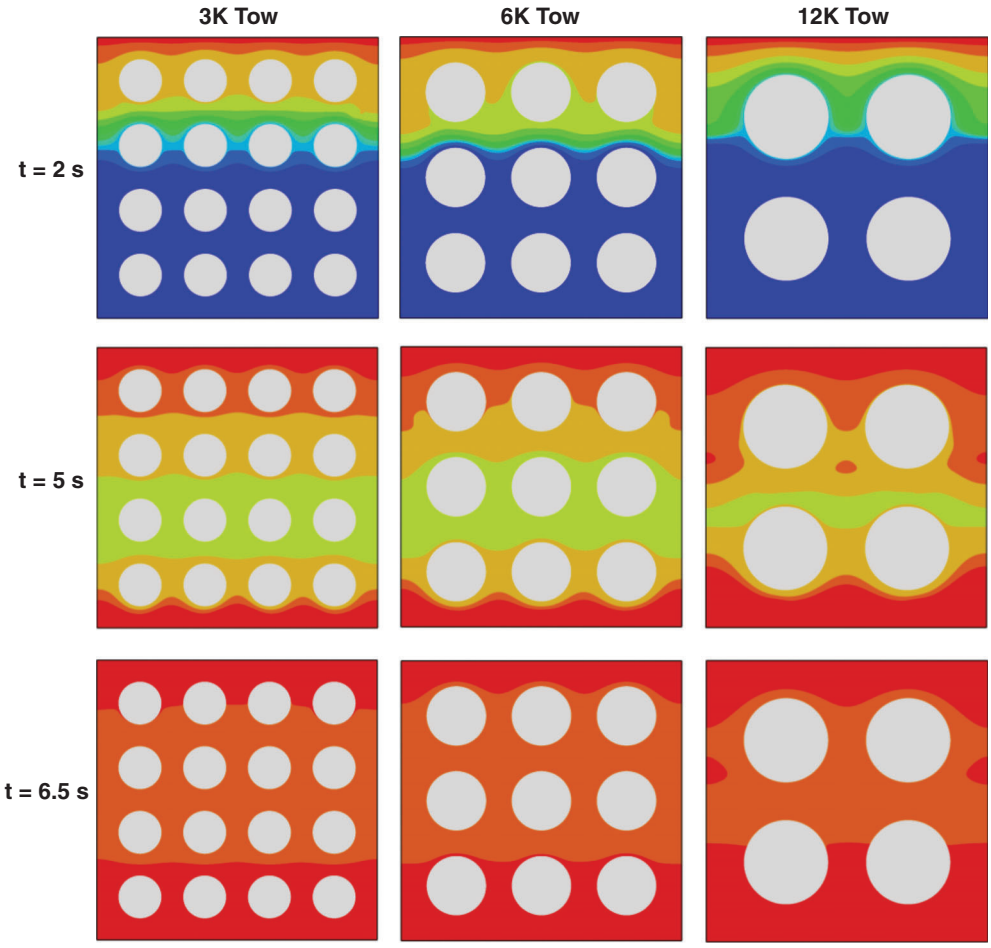

FIGURE 10 Comparison of the evolutions of the degree of cure field for unidirectional fiber composites with different fiber tow sizes, that is, 3 K, 6 K, and 12 K (the color legend is same with the one in Figure 6, where red denotes fully cured while blue denotes uncured). [Color figure can be viewed at wileyonlinelibrary.com]

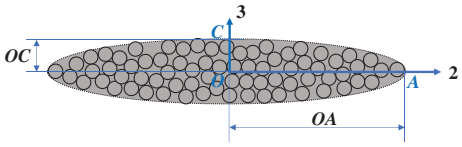

FIGURE 11 Schematic of the elliptical cross section of the fiber tow, where direction 2 represents the transverse direction and direction 3 represents the through-thickness direction of the composite laminate. [Color figure can be viewed at wileyonlinelibrary.com]

5.3 | Effect of tow size

Figure 10 illustrates the effect of the tow size. Specifically, it provides the comparison of the predicted evolution of the degree of cure for cases with different tow sizes, that is, 3, 6, and 12 K. The fiber volume fraction is fixed at 30%. The comparison reveals that the fiber tow size has an insignificant effect on the frontal polymerization process across the thickness. As we can see, for all cases, the polymerization front approximately propagates at the same pace across the thickness. Moreover, the "bottom-to-top" frontal polymerization can be observed in all cases. The only difference of the three cases is that the number of waves in the degree of cure contour along the horizontal direction is different, which is caused by the different number of fiber tows along the horizontal direction.

A quantitative comparison of the average front velocity and the maximum temperature for the fiber composites with fibers in different tow sizes is shown in Figure 9b. It can be noticed that the average front velocity drops by only 2.4% from 0.336 to 0.328 mm/s as the tow size increases from 3 to 6 K, and then, it slightly increases back from 0.328 to 0.334 mm/s as the tow size increase from 6 to 12 K. Overall, the effect of the fiber tow size on the average front velocity is insignificant. Furthermore, the maximum temperature during the frontal polymerization is also not much impacted by the change of the fiber tow size, as shown in Figure 9b. It varies between 336 and 343°C for cases with different fiber tow sizes, which gives a difference of only 2%. It is important to mention that the fiber tow in our simulations is modeled as a single solid fiber. In real situations, the fiber tow is a bundle of individual fiber filaments with the presence of voids between adjacent fiber filaments. The actual curing process also involves the curing

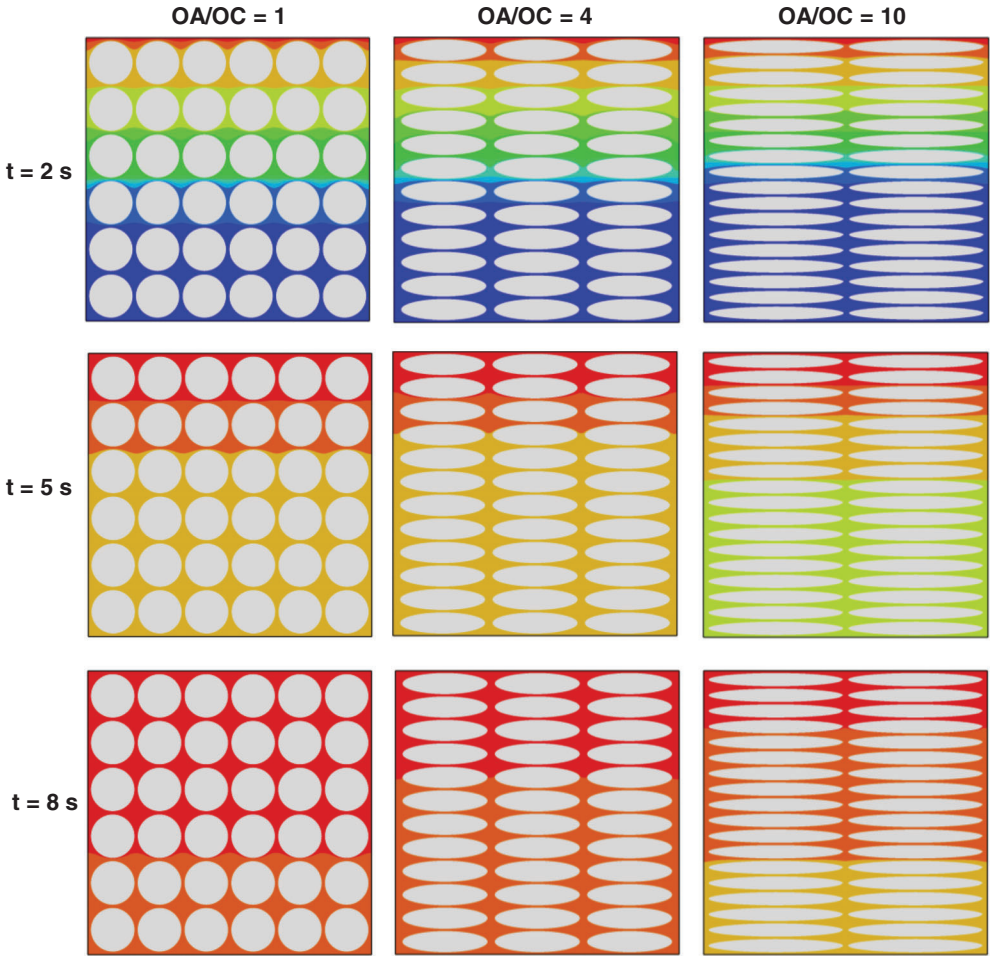

FIGURE 12 Comparison of the evolutions of the degree of cure field for unidirectional fiber composites with different fiber tow shapes, i.e., OA/OC = 1 (circular), OA/OC = 4, and OA/OC = 10 (the color legend is same with the one in Figure 6, where red denotes fully cured while blue denotes uncured). [Color figure can be viewed at wileyonlinelibrary.com]

from the outer perimeter of the fiber tow through the voids into the center of the fiber tow.[32] Such an intra-tow polymerization process is ignored in the current simulations and will be a subject of future investigations.

Additionally, as described earlier, the cross section of the fiber tow is idealized as a circular shape for simplicity in above simulation studies. According to Reference 33, the actual cross section of the fiber tow follows an approximate elliptical shape, as shown in Figure 11, where the major radius is denoted by OA and the minor radius is denoted by OC. To investigate the effect of the fiber tow shape on the frontal polymerization, simulation studies are conducted using fiber composites containing fiber tows with different ratios between OA and OC. The results are presented and discussed in the next section.

5.4 | Effect of tow shape

Figure 12 illustrates the comparison of the evolution of the degree of cure field in the fiber composites with different fiber tow shapes (i.e., OA/OC = 1, OA/OC = 4, and OA/OC = 10). Note that a fixed area of the elliptical cross sections of 0.12 mm^2 is used for all three cases, which represents the 3 K carbon fiber tow. Additionally, the fiber volume fraction of the three cases is fixed at 67%. Our simulation results show that the average front velocity decreases as the OA/OC increases. As shown in Figure 12, at the time of 8 s, more than half of the thickness of the fiber composites is fully cured for the case with OA/OC = 1, while only one third of the thickness and less than one fourth of the thickness is fully cured for cases with OA/OC = 4 and OA/OC = 10, respectively. Figure 9c provides the quantitative comparison of the average front velocity. As one can see, it decreases in an approximately linear trend as the OA/OC increases. Specifically, it decreases from 0.31 to 0.27 and 0.22 mm/s as the OA/OC increases from 1 to 4 and 10, respectively. The average front velocity is reduced by about 30% as the OA/OC increases from 1 to 10. Additionally, it can be noticed that the "bottom-to-top" frontal polymerization is not observed in all three cases, which implies that this effect is not related to the tow shape and is dependent on the fiber volume fraction (as discussed in Section 5.2). Figure 9c also shows that the maximum temperature stays at 220°C for all cases. The volumetric heat

generation does not cause the temperature to rise beyond 220°C due to the countering effect caused by the heat consumption in the carbon fibers.

6 | CONCLUSIONS

The effects of microstructure on the frontal polymerization process in the through-thickness direction of the unidirectional fiber composites are investigated in this article. The computational model employed to conduct the investigations is implemented using finite element analysis in ABAQUS with user heat flux HETVAL subroutine and user field USDFLD subroutine. The model is verified by comparing the predictions of the evolutions of the temperature field and the degree of cure with the experimental data for frontal polymerization in the DCPD resin. The parameters of the microstructures of unidirectional fiber composites investigated include the fiber volume fraction, fiber tow size, and the fiber tow shape. The main conclusions are as follows:

- The average front velocity significantly decreases by 58.0% as the fiber volume fraction increases from 0% to 30%, and then, it slowly decreases by 11.8% as the fiber volume fraction increases from 30% to 46%. Above 46%, the average front velocity plateaus.
- At lower fiber volume fractions (0%–46%), the volumetric heat quickly generates due to enthalpic reactions and accumulates at the bottom of the fiber composites, leading to the additional "bottom-to-top" frontal polymerization. At higher fiber volume fractions (>67%), the generation of the volumetric heat is countered by the increased heat consumption due to the heat conduction in the carbon fibers.
- The impact of the fiber tow size is insignificant on the average front velocity and the maximum temperature in the frontal polymerization in the through-thickness direction of the unidirectional fiber composites.
- The frontal polymerization is greatly affected by the shape of the fiber tow cross section. Assuming an elliptical cross section, the average front velocity approximately decreases linearly, as the ratio between the major axis and the minor axis increases. The reduction is about 30% when the ratio increases from 1 to 10.

The above findings generated from this study is expected to provide helpful guidance for the future scale-up of the frontal polymerization technology in the advanced manufacturing of thermoset fiber composites, including the rapid curing of thermoset resin for additive manufacturing and repair.

In addition to the factors investigated in this study, other factors, such as the weight fractions of the initiators and the uniformity of the dispersion of the initiators in the monomer can also influence the frontal polymerization process. These factors could result in changes in the thermal properties and the curing kinetics of the monomer mixture, thereby leading to different frontal polymerization behaviors. Furthermore, these factors may also affect the viscosity of the resin mixture, which results in changes in the capillary flow through the microstructure of the fiber tow, and hence in the intra-tow frontal polymerization process. These factors along with the fiber microstructures are expected to jointly determine the intra-tow frontal polymerization process due to the capillary effect and the permeability of the fiber tow, which merits further investigation.

ACKNOWLEDGMENTS

The author would like to acknowledge the financial support from the Collaboration for Unprecedented Success and Excellence (CUSE) Grant provided by the Syracuse University. The author also thanks Dr. Philippe H. Geubelle (Professor of Aerospace Engineering at University of Illinois at Urbana-Champaign) and Dr. Ian Hosein (Associate Professor of Biomedical and Chemical Engineering at Syracuse University) for many helpful discussions.

DATA AVAILABILITY STATEMENT

The HETVAL and USDFLD subroutines along with the ABAQUS input files, as well as datasets generated during and/or analyzed during the current study are available from the corresponding author on reasonable request.

ORCID

Yeqing Wang https://orcid.org/0000-0002-5673-9897

REFERENCES

[1] Solvay. Technical data sheet CYCOM® 977–3 epoxy resin, https://www.solvay.com/en/product/cycom-977-3.
[2] R. M. Jones, *Design of Composite Structures: An Introduction to the Many Aspects of Composite Structures Design*, Bull Ridge Publishing, Blacksburg, Virginia **2015**.
[3] R.A. Witik, F. Gaille, R. Teuscher, H. Ringwald, V. Michaud, J.-A. Månson. Assessing the economic and environmental potential of out of autoclave processing. 18th ICCM. **2011**.
[4] O. Uitz, P. Koirala, M. Tehrani, C. C. Seepersad, *Additive Manuf.* **2021**, *41*, 101919.
[5] M. G. B. Odom, C. B. Sweeney, D. Parviz, L. P. Sill, M. A. Saed, M. J. Green, *Carbon* **2017**, *120*, 447.
[6] K. Chen, X. Kuang, V. Li, G. Kang, H. J. Qi, *Soft Matter* **2018**, *14*, 1879.
[7] X. He, Y. Ding, Z. Lei, S. Welch, W. Zhang, M. Dunn, et al., *Additive Manuf.* **2021**, *40*, 101921.

[8] B. G. Compton, J. A. Lewis, *Adv. Mater.* **2014**, *26*, 5930.
[9] N. Nawafleh, E. Celik, *Additive Manuf.* **2020**, *33*, 101109.
[10] N. S. Hmeidat, J. W. Kemp, B. G. Compton, *Compos. Sci. Technol.* **2018**, *160*, 9.
[11] J. A. Pojman, V. M. Ilyashenko, A. M. Khan, *J. Chem. Soc., Faraday Trans.* **1996**, *92*, 2825.
[12] P. M. Goldfeder, V. A. Volpert, V. M. Ilyashenko, A. M. Khan, J. A. Pojman, S. E. Solovyov, *J. Phys. Chem. B.* **1997**, *101*, 3474.
[13] Q. Li, H.-X. Shen, C. Liu, C.-f. Wang, L. Zhu, S. Chen, *Prog. Polym. Sci.* **2022**, *127*, 101514.
[14] J. A. Pojman, *Cure-on-demand Composites by Frontal Polymerization, In Reference Module In Materials Science And Materials Engineering*, Elsevier, Amsterdam, Netherlands **2022**, p. 1.
[15] B. R. Groce, D. P. Gary, J. K. Cantrell, J. A. Pojman, *J. Polym. Sci.* **2021,** *59,*1678.
[16] A. D. Tran, T. Koch, R. Liska, P. Knaack, *Monatshefte für Chemie-Chemical Monthly.* **2021**, *152*, 151.
[17] E. Frulloni, M. M. Salinas, L. Torre, A. Mariani, J. M. Kenny, *J. Appl. Polym. Sci.* **2005**, *96*, 1756.
[18] A. D. Tran, T. Koch, P. Knaack, R. Liska, *Compos. Part A: Appl. Sci. Manufac.* **2020**, *132*, 105855.
[19] E. Goli, N. A. Parikh, M. Yourdkhani, N. G. Hibbard, J. S. Moore, N. R. Sottos, et al., *Compos. Part A: Appl. Sci. Manuf.* **2020**, *130*, 105689.
[20] I. D. Robertson, M. Yourdkhani, P. J. Centellas, J. E. Aw, D. G. Ivanoff, E. Goli, et al., *Nature* **2018**, *557*, 223.
[21] Y. Gao, S. Li, J.-Y. Kim, I. Hoffman, S. K. Vyas, J. A. Pojman, et al., *J. Nonlinear Sci.* **2022**, *32*, 013109.
[22] Y. Gao, F. Shaon, A. Kumar, S. Bynum, D. Gary, D. Sharp, et al., *J. Nonlinear Sci.* **2021**, *31*, 073113.
[23] S. Vyas, E. Goli, X. Zhang, P. H. Geubelle, *Compos. Sci. Technol.* **2019**, *184*, 107832.
[24] H. M. Yoo, M. S. Kim, B. S. Kim, D. J. Kwon, S. W. Choi, *e-Polymers.* **2019**, *19*, 437.
[25] G. Struzziero, B. Remy, A. A. Skordos, *J. Appl. Polym. Sci.* **2019**, *136*, 47015.
[26] M. E. Foley, J. W. Gillespie Jr., *J. Compos. Mater.* **2005**, *39*, 1045.
[27] Hexcel. HexTow® AS4 carbon fiber datasheet. https://www.hexcel.com/user_area/content_media/raw/AS4_HexTow_DataSheet.pdf.
[28] S. Lampkin, W. Lin, M. Rostaghi-Chalaki, K. Yousefpour, Y. Wang, J. Kluss. Epoxy resin with carbon nanotube additives for lightning strike damage mitigation of carbon fiber composite laminates. 34th Annual American Society for Composites Technical Conference, ASC 2019. Atlanta, GA. https://doi.org/10.12783/asc34/31338
[29] W. Lin, B. Jony, K. Yousefpour, Y. Wang, C. Park, S. Roy. Effects of graphene nanoplatelets on the lightning strike damage response of carbon fiber epoxy composite laminates. 35th Annual American Society for Composites Technical Conference, ASC 2020. Online. p. 1-15. https://doi.org/10.12783/asc35/34878
[30] A. Kumar, S. Roy, *Compos. Part B* **2018**, *134*, 98.
[31] W. Lin, Y. Wang, K. Yousefpour, C. Park, V. Kumar, *Appl. Compos. Mater.* **2022**, pp. *1-18*. https://doi.org/10.1007/s10443-022-10028-1
[32] T. A. Cender, P. Simacek, S. G. Advani, *Compos. Part A: Appl. Sci. Manufac.* **2013**, *53*, 118.
[33] X. Huang Mechanics and durability of fiber-reinforced porous ceramic composites. Ph.D. Thesis, Virginia Polytechnic Institute and State University **2002**.

How to cite this article: Y. Wang, *J. Appl. Polym. Sci.* **2022**, e52735. https://doi.org/10.1002/app.52735